Deformation of crystal surfaces in ferroelastic materials caused by antiphase domain boundaries

1997 J. Phys.: Condens. Matter 9 4583

(http://iopscience.iop.org/0953-8984/9/22/010)

J. Phys.: Condens. Matter **9** (1997) 4583–4592. Printed in the UK PII: S0953-8984(97)77918-9

Deformation of crystal surfaces in ferroelastic materials caused by antiphase domain boundaries

I Rychetský

Institute of Physics, Czech Academy of Sciences, Na Slovance 2, 18040 Prague, Czech Republic

Received 18 September 1996, in final form 3 March 1997

Abstract. The internal stresses occurring around domain walls can cause deformation of the crystal surface. The surface distortions have been calculated for the case of antiphase boundaries in tetragonal crystals. In KSCN a bump-shaped deformation of the surface occurs, with a height less than 1 Å. This effect is much smaller in Hg_2Br_2 but, besides a bump, a valley can also appear depending on the orientation of the antiphase boundary. The antiphase boundaries, the observation of which is difficult, could be revealed by such deformations of the crystal surface.

1. Introduction

Domain walls are very difficult to access because they are too narrow for most direct experimental methods. Ferroelastic domain walls (FDWs) can be visualized indirectly by polarized light which distinguishes the bulk domains. This is not so in the case of antiphase boundaries (APBs), since they separate two domains possessing identical tensorial properties. APBs are observed by destructive etching of the crystal surface [1, 2] or some other methods, e.g. x-ray topography [3] and electron microscopy [4–7]. It was recently shown that displacements of atoms in the APB centre result in internal strains localized around the APB plane [8–10]. One can naturally expect a bump-shaped deformation of the crystal surface in the vicinity of its intersection with the APB, owing to the relaxation of such stresses. The phenomenon described offers direct observation of APBs using scanning microscopy methods, but it will apparently depend on the magnitude of the surface distortion. We report here quantitative determination of the deformation, and its dependence on the temperature and on the orientation of domain wall, in the molecular crystals KSCN [2, 9] and Hg_2Br_2 [9].

The substances under consideration are improper ferroelastics undergoing a tetragonal-to-orthorhombic phase transition with the free-energy density [9]

$$f = f_0(p, q) + f_c(u_{ij}, p, q) + f_E(u_{ij}) + f_G(\partial_i p, \partial_i q) \tag{1}$$

with

$$f_0 = \tfrac{1}{2}\alpha(p^2 + q^2) + \tfrac{1}{4}\beta'(p^4 + q^4) + \tfrac{1}{4}\gamma' p^2 q^2$$
$$f_C = l_1'(p^2 + q^2)(u_{11} + u_{22}) + l_6'(p^2 - q^2)u_{12} + l_3'(p^2 + q^2)u_{33}$$
$$f_E = \sum c_{ijkl} u_{ij} u_{kl}$$
$$f_G = \tfrac{1}{2} g((\nabla p)^2 + (\nabla q)^2)$$

where p, q is the two-component order parameter (OP), f_0 is the pure OP part, f_C is linear-quadratic coupling between strains u_{ij} and the OP, f_E is a quadratic form of strains

0953-8984/97/224583+10$19.50

u_{ij} and f_G is a gradient term. The values of all coefficients of the free-energy expansion, which we use in our calculation, are for both crystals tabulated in [9]. The thermodynamic equilibrium state is represented by solution of the following system of equations [8]: the Lagrange–Euler equations

$$\frac{\mathrm{d}}{\mathrm{d}x_i}\frac{\partial f}{\partial(\partial p/\partial x_i)} - \frac{\mathrm{d}f}{\mathrm{d}p} = 0$$
$$\frac{\mathrm{d}}{\mathrm{d}x_i}\frac{\partial f}{\partial(\partial q/\partial x_i)} - \frac{\mathrm{d}f}{\mathrm{d}q} = 0 \qquad (2a)$$

and the equations of mechanical equilibrium given by

$$\partial_j \sigma_{ij} = 0 \qquad (2b)$$

where the stress components

$$\sigma_{ij} = \partial f/\partial u_{ij}. \qquad (2c)$$

Following the notation of Lechnickij [11],

$$\sigma_x = \sigma_{11} \qquad \sigma_y = \sigma_{22} \qquad \sigma_z = \sigma_{33} \qquad \tau_{xy} = \sigma_{12} \qquad \tau_{xz} = \sigma_{13} \qquad \tau_{yz} = \sigma_{23}$$

and

$$\epsilon_x = u_{11} = \partial U/\partial x \qquad \epsilon_y = u_{22} = \partial V/\partial y \qquad \epsilon_z = u_{33} = \partial W/\partial z \qquad (2d)$$
$$\gamma_{xy} = 2u_{12} = \partial U/\partial y + \partial V/\partial x \qquad (2e)$$
$$\gamma_{xz} = 2u_{13} = \partial U/\partial z + \partial W/\partial x \qquad (2f)$$
$$\gamma_{yz} = 2u_{23} = \partial V/\partial z + \partial W/\partial y \qquad (2g)$$

where (U, V, W) is the vector field of total displacements.

One should solve system (2) with appropriate boundary conditions with respect to the OP and the displacements (U, V, W).

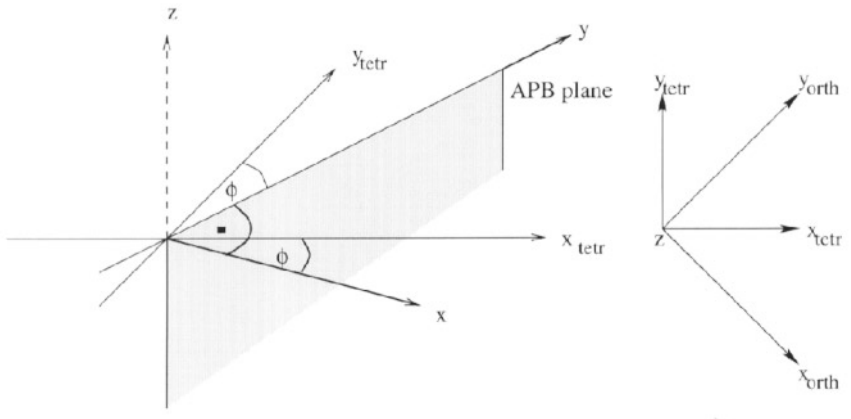

(a) (b)

Figure 1. (a) The APB plane is perpendicular to x and makes an angle ϕ with the tetragonal axes. (b) Tetragonal and orthorhombic axes.

2. Antiphase boundaries in a boundless crystal

Let us consider an APB denoted 1_1–1_2, between domains $1_1 = (-p_0, 0)$ and $1_2 = (p_0, 0)$. The APB plane is perpendicular to x and its orientation is characterized by the angle ϕ with respect to the tetragonal axis x_{tetr}, (figure 1). For the crystal extended to infinity (without surfaces), one obtains a kink-type solution for equations (2) [9]:

$$p(x) = p_0 \tanh(2x/d_{APB}) \tag{3}$$

with the position-independent strain components

$$\epsilon_z = \epsilon_z^\infty \qquad \epsilon_y = \epsilon_y^\infty \qquad \gamma_{yz} = 0 \tag{4}$$

and corresponding non-zero internal stresses σ_z and σ_y; the explicit form of the former is [9]

$$\sigma_z = (p^2 - p_0^2)\frac{A}{p_0^2}. \tag{5}$$

The magnitude $A \sim (T_C - T)$ and the wall thickness $d_{APB} \sim (T_C - T)^{-1/2}$ also depend on the orientation of APB (figure 2). The remaining components of the stress tensor are zero. The analytical expressions for A and d_{APB} were obtained in [9].

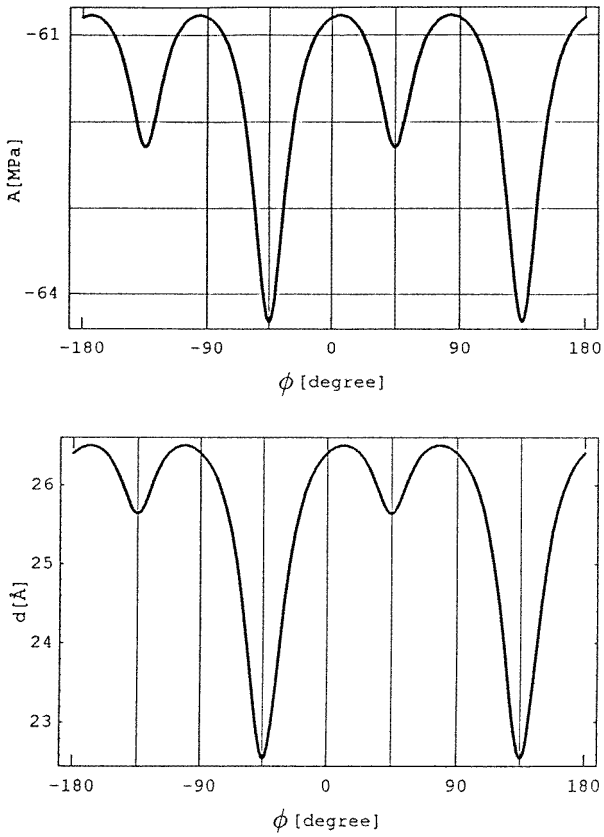

Figure 2. The angular dependence of the APB thickness $d = d_{APB}$ and the amplitude A of the internal stress component σ_z for $T = T - 5$ K in KSCN.

3. Intersection of an antiphase boundary with the surface

Let us assume a semi-infinite crystal with the upper surface being the tetragonal plane perpendicular to the z axis. The solution (3)–(5) obtained for the infinite crystal is again valid in the half-space $z \leqslant 0$, provided that an external position-dependent stress equal to σ_z inserted at $z = 0$ keeps the crystal surface planar. The stress-free surface is obtained by the insertion of the opposite stress component [12, 13]

$$p_z = -\sigma_z = \frac{A}{\cosh(2x/d_{APB})^2} \tag{6}$$

at $z = 0$. For simplicity, we assume the profile (3) to be unchanged up to the surface, i.e. only the elastic term f_E in (1) is considered. Then the elastic properties are described by the bare elastic moduli (the components s_{ij} referred to the tetragonal system, or $a_{ij}(\phi)$ in the coordinates x, y, z rotated at an angle ϕ).

Our aim is now to calculate the deformation of the planar crystal surface loaded with the stress (6). The problem can be analytically treated by using an approximate algebraic expression instead of (6) [9]:

$$p_z = A\frac{c^4}{(c^2 + x^2)^2} \qquad c = \frac{2d_{APB}}{\pi}. \tag{7}$$

The solution of the two-dimensional problem, in which all quantities depend on y and z only, can be solved using the method worked out by Muschelischvili [14] and for the anizotropic case by Lechnickij [11]. Following Lechnickij we introduce the reduced elastic moduli

$$\beta_{ij} = a_{ij} - a_{i2}a_{j2}/a_{22} \qquad i, j = 1, 3, 4, 5, 6. \tag{8}$$

The characteristic equation

$$l_4(\mu)l_2(\mu) - l_3(\mu)^2 = 0 \tag{9}$$

with

$$\begin{aligned} l_4(\mu) &= \beta_{11}\mu^4 + (2\beta_{13} + \beta_{55})\mu^2 + \beta_{33} \\ l_3(\mu) &= \beta_{16}\mu^3 \\ l_2(\mu) &= \beta_{66}\mu^2 + \beta_{44} \end{aligned}$$

has six complex roots $\mu_1, \mu_2, \mu_3, \mu_1^*, \mu_2^*, \mu_3^*$, and one defines also

$$\lambda_1 = -l_3(\mu_1)/l_2(\mu_1) \qquad \lambda_2 = -l_3(\mu_2)/l_2(\mu_2) \qquad \lambda_3 = -l_3(\mu_3)/l_4(\mu_3). \tag{10}$$

The complex stress functions can be easily calculated (the isotropic case was studied in [12]):

$$\begin{aligned} \Phi_1'(z_1) &= -\frac{Ac}{4}\frac{\mu_3\lambda_2\lambda_3 - \mu_2}{\Delta}\frac{2c + \mathrm{i}z_1}{(z_1 - \mathrm{i}c)^2} \\ \Phi_2'(z_2) &= -\frac{Ac}{4}\frac{\mu_1 - \mu_3\lambda_1\lambda_3}{\Delta}\frac{2c + \mathrm{i}z_2}{(z_2 - \mathrm{i}c)^2} \\ \Phi_3'(z_3) &= -\frac{Ac}{4}\frac{\mu_2\lambda_1 - \mu_1\lambda_2)}{\Delta}\frac{2c + \mathrm{i}z_3}{(z_3 - \mathrm{i}c)^2} \end{aligned} \tag{11}$$

where $\Delta = \mu_2 - \mu_1 + \lambda_2\lambda_3(\mu_1 - \mu_3) + \lambda_1\lambda_3(\mu_3 - \mu_2)$ and $z_k = x + \mu_k z = x + zn_k + \mathrm{i}zm_k$, $n_k = \mathrm{Re}[\mu_k]$, $m_k = \mathrm{Im}[\mu_k]$, $k = 1, 2, 3$. Do not confuse the complex 'coordinates' z_k and the real coordinate z.

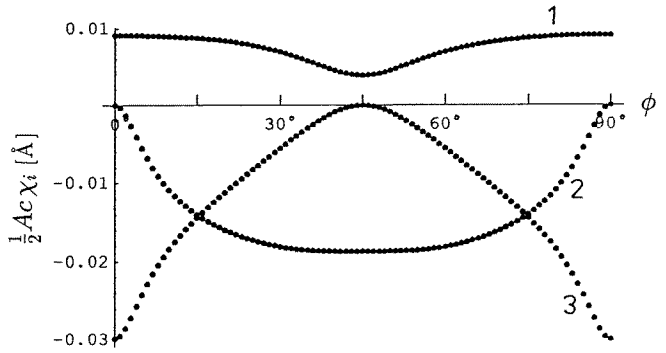

(a)

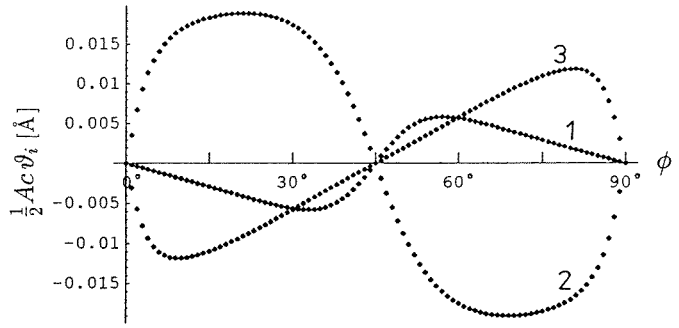

(b)

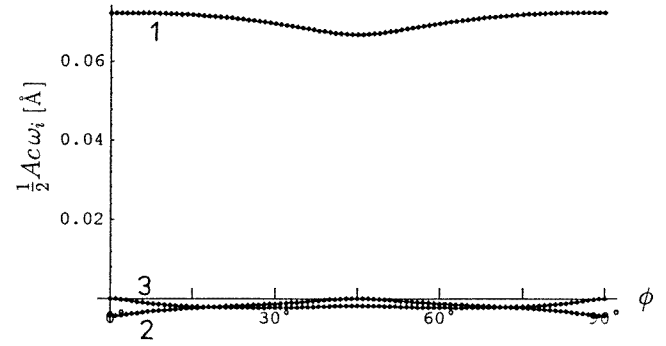

(c)

Figure 3. The angle-dependent coefficients in equation (12) for KSCN at $T = T_C - 5$ K: (a) $\chi_i Ac/2$ (Å), $i = 1, 2, 3$; (b) $\vartheta_i Ac/2$ (Å), $i = 1, 2, 3$; (c) $\omega_i Ac/2$ (Å), $i = 1, 2, 3$; (d) m_i, $i = 1, 2, 3$.

4. Crystal line KSCN

The material constants used are available in our previous paper [9]. By an inspection of equation (9), which is the cubic equation with respect to μ^2, it turns out that all roots are

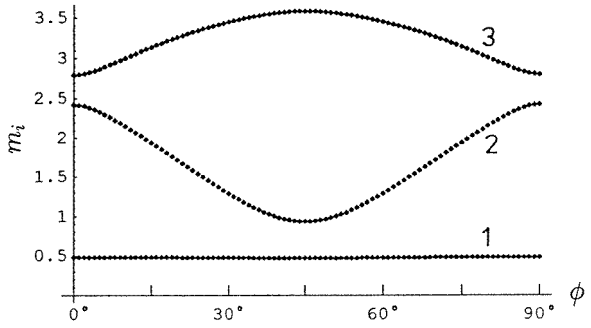

(d)

Figure 3. (Continued)

purely imaginary for KSCN, i.e. $n_k = 0$, $k = 1, 2, 3$. Then the displacements are

$$U(x,z) = \frac{Ac}{2}\sum_{i=1}^{3}\chi_i(\phi)\left[\frac{cx}{x^2+(c-m_iz)^2} + \tan^{-1}\left(\frac{x}{c-m_iz}\right)\right]$$
$$W(x,z) = \frac{Ac}{2}\sum_{i-1}^{3}\omega_i(\phi)\left[\frac{c(c-m_iz)}{x^2+(c-m_iz)^2} - 1 + \tfrac{1}{2}\ln\left(\frac{x^2+(c-m_iz)^2}{c^2}\right)\right] \qquad (12)$$
$$V(x,z) = \frac{Ac}{2}\sum_{i=1}^{3}\vartheta_i(\phi)\left[\frac{cx}{x^2+(c-m_iz)^2} + \tan^{-1}\left(\frac{x}{c-m_iz}\right)\right]$$

where the angle-dependent coefficients $\chi_i(\phi)$, $\omega_i(\phi)$, $\vartheta_i(\phi)$ and $m_i(\phi)$ depend on the elastic moduli. Instead of complicated explicit formulae we have plotted them in figure 3. The distortion of the surface that one obtains by putting $z = 0$ in equations (12) and its 3D plot is shown in figure 4. Of course, it depends on the orientation of the APB. The displacement W along the z axis consists of a rapidly decaying algebraic part and a gradually descending logarithmic term. In figure 5, we show the displacement W in the APB centre $x = 0$ referred to W at the distance $x = 10c$, where the algebraic term becomes small. Note that the temperature-dependent quantities are A and d_{APB} only and the figures are drawn for the temperature $T = T_C - 5$ K. From figures 4 and 5 it follows that the deformation has a bump shape of typical height about 0.2 Å and width about 10 nm, which depend only weakly on the APB orientation.

5. Crystalline Hg_2Br_2

In the case of mercury bromide, equations (12) are again valid in a wide range of angles. In the small intervals 37–43° and 49–55° the roots μ_k, $k = 1, 2, 3$, are complex with a non-zero real part and then the equations for the displacements become more complicated. In figures 6 and 7 the angle-dependent wall thickness and the amplitude of the stress component σ_z respectively are plotted [9]. In figure 8 the deformation of the crystal surface is shown, for the angle 45°. The angle-dependent displacement $W(x = 0, z = 0)$ of the intersection of the APB and the surface, referred to the displacement $W(x = 10c, z = 0)$, is drawn in figure 8. The distance $10c = 20d_{APB}/\pi$ of the reference point also depends on the angle and typically reads about 1500 Å. The main difference from KSCN is the very small distortion of the surface. Besides the bump occurring for negative A, there exists a range

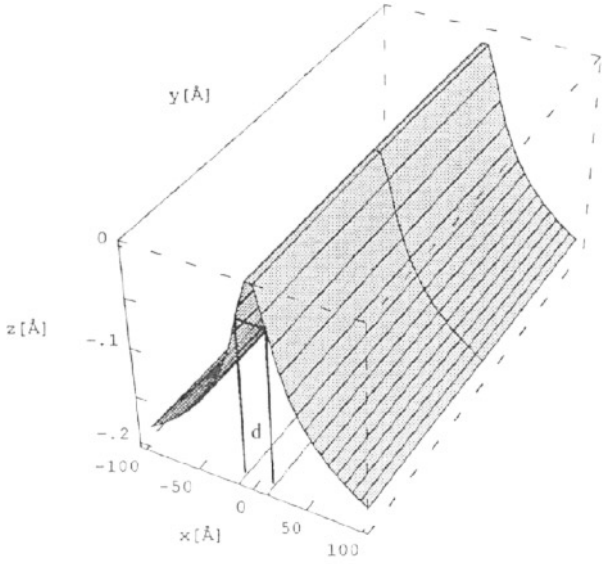

Figure 4. Deformation of the crystal surface in KSCN, for the angle $\phi = 0^\circ$ and $T = T_C - 5$ K. The APB plane is $x = 0$ and its thickness is denoted by d.

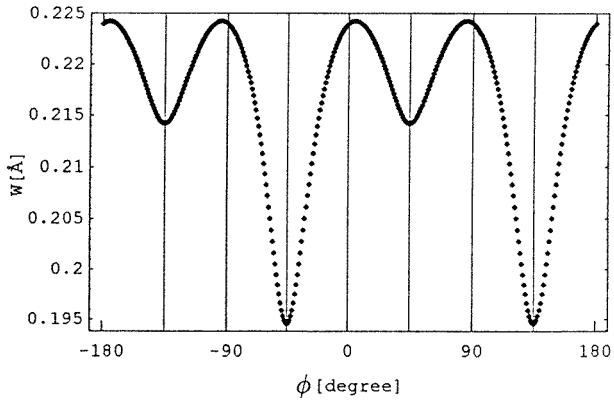

Figure 5. Angular dependence of the surface distortion (displacement W) parallel to z in the APB centre ($x = 0$), counting from the displacement W at the distance $x = 10c$ (i.e. about 150 Å).

of angles with positive A and a valley-shaped deformation of the surface (figures 6–8). The amplitude of the surface deformation is extremely small in comparison with KSCN, approaching only several hundredths of an Ångström.

6. Conclusions

We have estimated the deformation of the crystal surface caused by the presence of the APB in the anisotropic materials. First, the bulk crystal was considered and the APB structure and internal stresses were obtained using a standard Landau approach. Then it was assumed

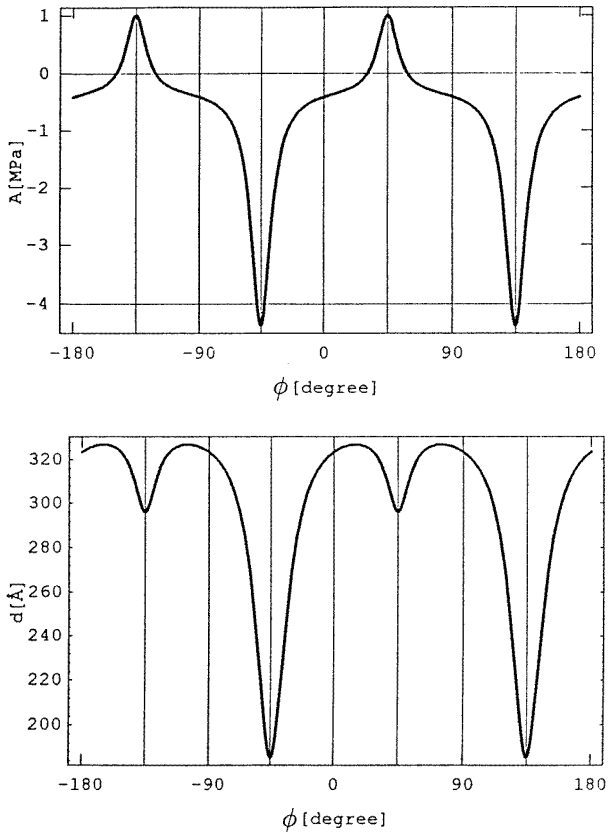

Figure 6. The angular dependence of the APB thickness $d = d_{APB}$ and the amplitude A of the internal stress component σ_z in Hg_2Br_2 for $T = T_C - 5$ K.

that in the semi-infinite crystal the structure of the APB near the surface is the same as in the bulk. Under such an assumption it was possible to calculate analytically the deformation of the surface corresponding to the release of internal stresses. The approximations made should be noted. Firstly, the constant APB profile up to the (undeformed planar) surface is reasonable for the long-range forces occurring in ferroelectrics and ferroelastics. We do not consider situations which would change this simple characteristic of the surface, e.g. extra atoms deposited at the surface or surface reconstruction. Secondly, the surface deformation caused by the internal stresses should reversibly cause a change in the APB profile near the surface due to the coupling of the OP and strain tensor in the free energy. In other words we should minimize the free energy with respect to both the deformations and the OP, but that would lead to a complicated 3D problem. For simplicity the APB profile was kept fixed all the time and only the elastic part of the free energy was minimized. This means that the results obtained overestimate real deformations, but corrections are assumed to be small [12].

Two materials KSCN and Hg_2Br_2 were quantitatively analysed. In KSCN the bump-shaped distortion of the surface depends on the APB orientation. The angular dependence of the bump's height (figure 5) is in accord with the etched pattern observed in [2, 15].

Its typical height at $T = T_C - 5$ K is rather small, about 0.2 Å and its width is more

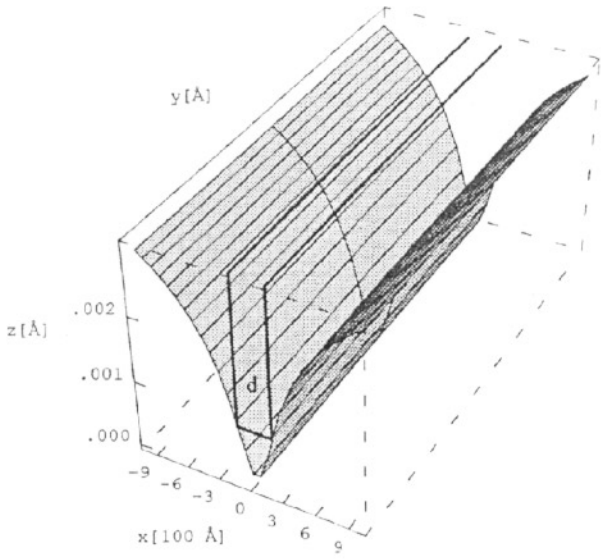

Figure 7. Deformation of the crystal surface in Hg_2Br_2, at $\phi = 45^\circ$ and $T = T_C - 5$ K. The APB plane is $x = 0$ and its thickness is denoted by d.

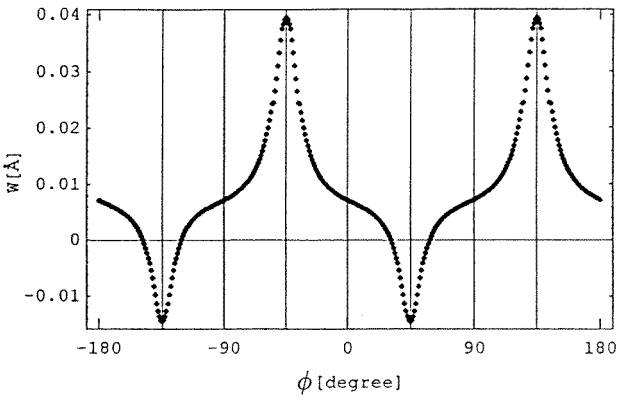

Figure 8. Angular dependence of the surface distortion W parallel to the z axis in the APB centre ($x = 0$), counting from the distortion W at the distance $x = 10c$ (i.e. about 1500 Å).

than 10 nm (figure 4). Owing to the linear temperature dependence, our formulae give a height of nearly 1 Å at $T = T_C - 25$ K. Since this value is a fraction of the lattice constant, the lattice defects (such as steps at the surface) dominate the deformations coming from the boundaries. Therefore the observation of such a tiny effect requires a molecularly flat and perfect crystal surface, and the high resolution of scanning methods [16]. Recently great progress has been made in this field. Ferroelectric domains and domain boundaries have been observed at the perfect surface of a TGS crystal by the atomic force microscopy (AFM) method [17, 18]. The topographic resolution (vertical to the surface) was 0.5 Å and it could even reach 0.1 Å. The horizontal resolution was about 8 nm. Comparing this with

the calculated example of KSCN we conclude that the surface deformation caused by the APB could be large enough to be observed by AFM. Of course such crystal must have a perfect surface. Let us assume that there are still a certain number of point defects, which also deform the surface. The deformation of the point defect has the shape of an isolated mountain and it can be in principle distinguished from the roof-like distortion (figure 4) caused by the APB.

In the case of Hg_2Br_2 the deformation of the surface possesses the shape of a bump or a valley depending on the APB orientation, but its magnitude is extremely small.

Since the stresses in FDW and APB are comparable [9, 10, 19], deformation of the same order should also appear around the intersection of the FDW with the surface. However, this tiny effect will be masked by strains arising from the matching of the bulk ferroelastic domains [20].

Acknowledgments

The author sincerely thanks J Fousek for stimulating comments.

This work was supported by the Grant Agency of the Czech Republic under project 202/95/1393.

References

[1] Barkley J R and Jeitschko W 1973 *J. Appl. Phys.* **44** 938
[2] Schranz W, Streuselberger T, Fuith A, Warhanek H and Götzinger M 1988 *Ferroelectrics* **88** 136
[3] Capelle B and Malgrange C J 1982 *Appl. Phys.* **53** 6762
[4] van Landuyt J, Gevers R and Amelinckx S 1964 *Phys. Status Solidi* **7** 519
[5] Humphreys C J, Howie A and Booker G R 1967 *Phil. Mag.* **15** 507
[6] Renault N A, Penisson J M and Bourret A 1973 *Phil. Mag.* **28** 103
[7] Yamamoto N, Yagi K and Honjo G 1977 *Phys. Status Solidi* a **44** 147
[8] Cao W and Barsch G R 1990 *Phys. Rev.* B **41** 4334
[9] Rychetský I and Schranz W 1993 *J. Phys.: Condens. Matter* **5** 1455
[10] Rychetský I 1995 *Ferroelectrics* **172** 105
[11] Lechnickij S G 1977 *Theory of Elasticity of Anisotropic Bodies* (Moscow: Nauka) (in Russian)
[12] Kroupa F and Vagera I 1969 *Czech. J. Phys.* B **19** 1204
[13] Rieder G 1959 *Abh. Braunschw. Wiss. Ges.* **11** 20
[14] Muschelischvili N I 1966 *Some Basic Problems of Mathematical Theory of Elasticity* (Moscow: Akademii SSSR Nauk) (in Russian)
[15] Schranz W and Rychetský I 1993 *J. Phys.: Condens. Matter* **5** 3871
[16] van de Leemput L E C and van Kempen H 1992 *Rep. Prog. Phys.* **55** 1165
[17] Eng L M, Fousek J and Guenter P 1997 *Ferroelectrics* in press
[18] Fousek J private communication
[19] Rychetský I and Schranz W 1994 *J. Phys.: Condens. Matter* **6** 11 159
[20] Schranz W, Rychetský I and Warhanek H 1993 *Ferroelectrics* **141** 61